Appl. Phys. B 78, 299–304 (2004)
DOI: 10.1007/s00340-003-1381-6

Applied Physics B
Lasers and Optics

C. CORSI[1]
A. TORTORA[1,2]
M. BELLINI[2,✉]

Generation of a variable linear array of phase-coherent supercontinuum sources

[1] European Laboratory for Non Linear Spectroscopy (L.E.N.S.), Via N. Carrara 1, 50019 Sesto Fiorentino (FI), Italy
[2] Istituto Nazionale di Ottica Applicata, L.go E. Fermi 6, 50125 Firenze, Italy

Received: 12 September 2003 /
Revised version: 12 November 2003
Published online: 3 February 2004 •

ABSTRACT We investigate the coherence properties of a linear array of white-light sources produced in bulk media by ultrashort laser pulses. The array is generated out of the spatial interference pattern between two laser pump pulses, so that the number of supercontinuum sources and their separations can be easily manipulated by varying the geometry of the laser beam interaction. We find that all the secondary white-light sources which arise from the generation of filaments in the optical medium are well phase-locked and are thus able to generate stable and high-visibility multiple-beam interference patterns in the far-field. Observations are compared to the results of a simple model which takes into account a clamping of the peak laser intensity inside the filaments and includes intensity-dependent phase shifts among the different sources.

PACS 42.65.Jx; 42.65.Ky; 42.65.Re

1 Introduction

Since the first observations in the late 1960's [1], the phenomenon of supercontinuum generation, i.e. the extreme spectral broadening resulting in the generation of white light when ultrashort and powerful laser pulses propagate in a transparent medium, has been demonstrated in a variety of materials, including solids, liquids [2], and gases [3, 4]. Its broadband and ultrashort characteristics make it a unique light source [5, 6] for applications, and it is now routinely used for femtosecond time-resolved spectroscopy [7, 8], in optical pulse compression for the generation of ultrashort pulses [9, 10], or as a seed pulse of optical parametric amplifiers [11–13].

Continuum generation results from a complex interplay of self-phase-modulation [1, 2, 14], self-focusing [3, 15], and several other nonlinear optical effects. The collapse of the beam profile due to self-focusing is one of the main ingredients for the generation of the continuum when the power of the pump pulse reaches a critical threshold. Experiments have indeed shown that the threshold for supercontinuum generation corresponds to the calculated critical value for self-focusing [3, 4, 15, 16]. It has been demonstrated that when intense ultrashort laser pulses are focused in transparent media, they tend to break up into a number of intense filaments [17–19], and due to the competition between focusing by the Kerr effect and defocusing by free electrons (created in multiphoton or avalanche ionization), the diameter of these filaments and the peak laser intensity inside them tend to remain constant against increasing input pulse energies [20].

The combined action of the highly nonlinear phenomena involved in the generation of supercontinuum might lead to the conclusion that even small perturbations in the conditions of interaction with the medium can strongly affect the amplitude and phase properties of the white-light pulses. In particular, one may expect that small intensity variations in the pump pulses or small inhomogeneities in the materials may lead to dramatic phase and intensity fluctuations in the generated supercontinua.

Recently, it has been demonstrated that the phase coherence of the pump pulses can however be preserved in the process of supercontinuum generation [21], and a wealth of new work culminating in the realization of the so-called femtosecond frequency combs, are now revolutionizing the fields of high-precision spectroscopy and metrology [22–25]. When a regular train of phase-locked ultrashort laser pulses (such as those emitted by a mode-locked laser) is used to produce a train of collinear and phase-locked supercontinuum pulses, the comb of modes (spaced by the known laser repetition rate) which constitutes its spectrum can be used as a ruler in the spectral domain to measure large frequency differences with extremely high precision. Supercontinuum generation is a convenient way to easily broaden laser pulse spectra to more than an optical octave and the coherent nature of the supercontinuum generation process is essential to ensure that the comb spectral structure of the mode-locked laser is transferred to the white-light continuum.

The first experiments dealing with the mutual coherence of supercontinuum pulses were performed with amplified laser systems in bulk media, demonstrating that spatially separated white-light sources could exhibit high-visibility spatial interference fringes [21, 26, 27] and that the phase of the laser pump pulses was preserved in the generation process. Recently, a reduced version of the frequency-comb configuration was demonstrated by proving the mutual coherence of

✉ Fax: +390-55/457-2451, E-mail: bellini@ino.it

collinear, time-delayed pairs of supercontinuum sources generated in bulk materials and showing the appearance of clear and robust spectral interference fringes [28].

In this work we demonstrate the spatial-domain analog of the frequency-comb method by generating a linear array of equally spaced supercontinuum sources in a bulk material and proving their high degree of mutual coherence. The spatial characteristics of the array can be easily manipulated by varying the geometry of the pump pulse interaction and a simple method, based on the observation of the far-field interference patterns generated by the array, is used to investigate the mutual coherence of the white-light sources. Multiple supercontinuum sources require a stringent relative-phase stability in order to produce a stable and clear interference pattern. Our results show that this can be simply achieved, and we observe the spatial counterpart of a stable frequency-comb as an array of equally-spaced interference peaks in the far-field. The experimental interference patterns are well reproduced by a simple model including an intensity-dependent phase shift for the different supercontinuum sources.

2 Experimental

The pump laser for the experiments is an amplified Ti : sapphire system (Femtolasers, Femtopower PRO) delivering 0.8-mJ, 30-fs pulses centered around 780 nm at a repetition rate of 1 kHz. A Michelson interferometer is used to split the laser pulses into two equally intense replica and to vary their relative delay. By properly adjusting the angle of one of the folding mirrors of the interferometer, it is possible to change the angle between the outgoing laser pulses and produce straight interference fringes of variable period in the zone of beam crossing. A cylindrical lens with a focal length of 150 mm is placed after the Michelson interferometer (with its focal plane coincident with the beam crossing region) in order to focus the outgoing pulses along a direction orthogonal to the plane containing the laser beams. In such a configuration the straight interference fringes are compressed down to between 10 and 20 microns in one dimension while the spacing and the width of the spots in the other dimension can be simply adjusted by changing the relative angle between the two beams.

Glass and quartz plates of different thickness (ranging from 2 to 10 mm) are placed in the focus position, and the regions of high intensity corresponding to the maxima of the interference fringe pattern become the sources for the emission of supercontinuum. The laser pulse energy is varied in order to reach the threshold for white light generation from many consecutive interference maxima. Even at the highest intensities available with our laser system, supercontinuum generation from the different sources in the array always proceeds through the formation of a single filament and multiple filamentation from a single source is never observed. From previous investigations and experimental results from different groups, we estimate the peak laser intensity in each source region to be around 10^{12}–10^{13} W/cm^2.

After the interaction region, the supercontinuum pulses are left free to propagate towards a screen where they form a complex interference pattern. The fringe system can be studied by scanning a photomultiplier, apertured by a 35-μm diameter pinhole, along a direction perpendicular to the fringes by means of a computer-controlled translation stage. Colored filters are placed in front of the detector to select different spectral regions in the visible continuum. In order to study the near-field region inside the transparent material, the source area is also imaged on a distant screen and magnified (by a factor of about 40) by means of a lens.

3 Results and discussion

Let us refer to Fig. 1, where the geometry of the interaction is illustrated. The two laser beams intersect with an angle 2α and we assume that the delay between the two arms of the interferometer is adjusted so that the pulses cross the plane $x = 0$ at the same time. We also assume that the plane $y = 0$ corresponds to the focal plane of our cylindrical lens and coincides with the plane of maximum beam overlap perpendicular to the bisector of the two propagation vectors. In this case, the different positions along the x axis simply map different relative delays τ between the arrival time of the two pulses at the position $(x, 0)$ as:

$$\tau(x) = 2\frac{x}{c}\sin(\alpha) \tag{1}$$

If the coherence time of the laser pulses is τ_c (we will assume that we are dealing with Fourier transform-limited pulses, with a pulse duration equal to $\tau_c \approx 30$ fs, in the rest of the paper) then one can expect to observe an interference fringe pattern of good visibility for a spatial extension of about

$$\Delta x_c \simeq \frac{c\tau_c}{2\sin(\alpha)} \tag{2}$$

and with a fringe period of

$$\Delta x_p = \frac{\lambda}{2\sin(\alpha)} \tag{3}$$

So, by varying the angle α it is easily possible to change the dimensions of the source area and the fringe spacing in

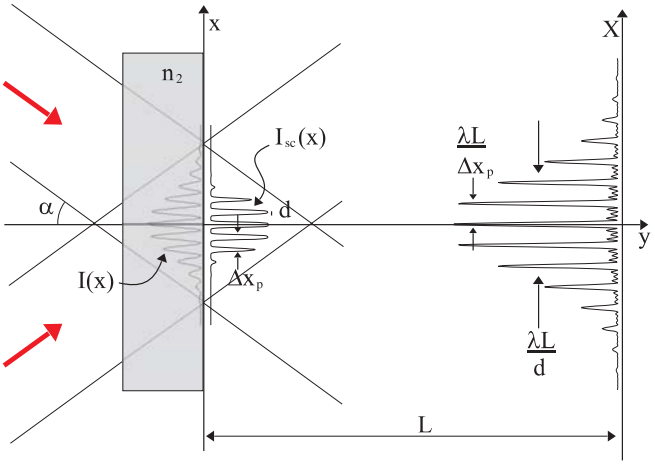

FIGURE 1 Sketch of the experimental setup illustrating the geometry of the interaction. Two laser pulses intersect at an angle α and form an interference pattern on the x plane inside the material. The maxima of this interference pattern become the sources for supercontinuum radiation which propagates to a screen placed at a distance L

a wide interval. Increasing α to a maximum value of about 1×10^{-2} rad could result in the generation of an extremely dense interference pattern, less than 500 μm wide, and with an inter-fringe spacing of just 40 μm. Note that in all cases, the total number of fringes in the array is constant, and is independent from the angle between the beam directions and of the order of 10–20.

In the following we will assume that α is large enough to ensure that the region of pulse interference is much smaller than the beam width along the x direction. This allows neglecting of the spatial distribution of the pump intensity and consideration of the simple interference of two plane waves along this axis. The two-pulse pump intensity distribution $I(x)$ in the $y = 0$ plane can be simply found if we also assume that the two laser pulses are of a Gaussian shape in time and have the same peak intensity I. In this case

$$I(\tau) = 2I(1 + V(\tau)\cos(\omega\tau)) \tag{4}$$

where the fringe visibility $V(\tau)$, defined as $\frac{I_{\mathrm{Max}} - I_{\mathrm{min}}}{I_{\mathrm{Max}} + I_{\mathrm{min}}}$, is given by

$$V(\tau) = \mathrm{e}^{-(\frac{\tau}{\tau_c})^2 \ln 2} \tag{5}$$

and one can make use of (1) to convert the time delays into a transverse spatial position.

An independent measurement has been carried out on a simpler setup with a spherical lens and a single beam in order to record the evolution of the different spectral components of the supercontinuum in a single filament as a function of the laser pulse energy. We have found a general behavior similar to the one reported in Fig. 2 for the region around 550 nm. No significant spectral broadening occurs up to a well defined value of the incoming pulse energy (about 0.32 μJ in this case), where a sharp increase in generation efficiency takes place followed by a saturation. The explanation of this behavior is connected to modifications in the spatial profile of the pulses due to self-focusing. At low power the pulses do not suffer sufficient self-phase-modulation to significantly broaden their spectrum, at some point they reach the critical power for self-trapping and the intensity in the so-formed filament suddenly increases and gives rise to the new spectral components in the visible region. Experimental values in the 5–10 MW range for the threshold power of supercontinuum formation agree well with the calculated critical power for the onset of self-focusing and indicate the close connection between the two phenomena.

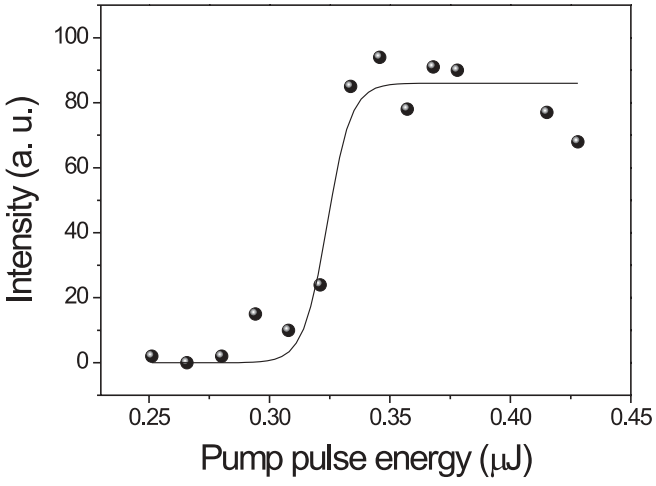

FIGURE 2 Behavior of the supercontinuum intensity variation as a function of the incoming laser power for a wavelength of about 550 nm. *Filled circles* are experimental data while the *solid line* is a fit with the hyperbolic tangent function (6) used to model this behavior

In order to simulate the process of white light generation in the case of our multiple-source arrangement, we model the supercontinuum intensity dependence on the pump intensity as:

$$I_{\mathrm{SC}}(x) \propto 1 + \tanh\left(\frac{I(x) - I_{\mathrm{th}}}{\Delta I}\right) \tag{6}$$

with the threshold intensity I_{th} and the transition interval ΔI adjusted to mimic the experimental results in the different cases, as shown by the solid line in Fig. 2. Although the hyperbolic tangent function of (6) is just a mathematical tool to model the sudden appearance of supercontinuum in a very simple way, the threshold intensity I_{th} has an evident connection with the onset of beam self-focusing and with the formation of a filament in the medium. Indeed, the threshold intensities used to simulate the experimental results normally range between a few times 10^{11} and 10^{12} W/cm^2, and these values are again in good agreement with the expected critical power for self-focusing, once the area of each interference maximum (that we roughly consider as an elliptical spot with radii depending on the particular experimental geometry) is taken into account.

It is also clear that the number N of supercontinuum sources (and consequently, the spatial extension of the array) is a directly controllable parameter via control of the pump pulse energy. High laser power allows generation from many spatially-separated sources, while lower power limits the production of white light to only a few central interference maxima. By varying the pump pulse energy, the number of supercontinuum sources was changed from 3-4 to as many as 40 when the full laser power also allowed self-focusing for interference maxima in the extreme wings of the pattern.

Figure 3 shows a near-field image, taken with a CCD camera, of the interaction region, where many equally-spaced sources of white light are clearly visible. In this case the angle α was adjusted to a value of about 5×10^{-3} rad and the extension of the array was measured to be about 1 mm, with an inter-source spacing of 75 μm. An horizontal cut of this figure (shown in the middle plot of Fig. 3) indicates that the central part of the pump interference pattern produces supercontinuum secondary sources of almost constant intensity despite the Gaussian profile of $I(x)$. The bottom plot in Fig. 3 shows that, by using (6) to cut the low-intensity pump regions and to saturate the interference maxima, it is possible to reproduce the intensity distribution of the white-light sources in a very reasonable way.

The next point is to evaluate the mutual phase coherence among the white-light sources in the array. As a first observation, one should note that if the different sources emit white light with a random relative phase and if such phase distribution varies from shot to shot, then they are not able to produce any visible interference pattern in the far field and

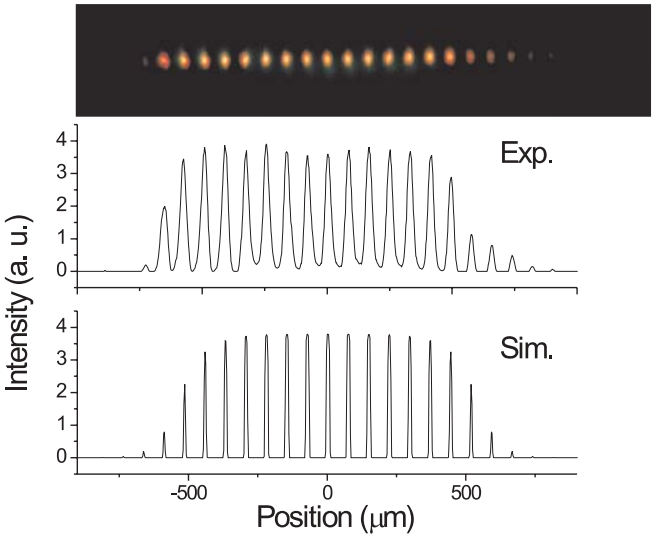

FIGURE 3 Experimental CCD image of the supercontinuum array source region. Also reported are the profiles obtained by a horizontal cut across the image and the simulated supercontinuum intensity distribution from (4), (5), and (6). An array of about 15 white-light sources of almost constant intensity is produced in this case

only a smooth intensity distribution is expected when time-averaged observations are performed. If, on the other hand, the phase distribution among the different supercontinuum sources is still random but does not change from a laser shot to the next one, then some form of irregular interference pattern will be evident on the screen. Finally, if the phase distribution among the sources is constant or has some smooth and regular behavior, then a clear periodic interference pattern will be present. As an example to illustrate this situation, one can consider the simple interference pattern produced by a linear array of N, equally spaced (by a distance Δx_p), and phase-locked, infinitesimal sources. The textbook solution for this problem is given by the expression:

$$I(\theta) = I_0 \left(\frac{\sin N\theta/2}{\sin \theta/2} \right)^2 \tag{7}$$

where θ is the phase delay between consecutive sources as seen from a point on the screen. In the limit of large screen distance L and small source extension, the phase at a transverse position X of the screen is:

$$\theta(X) \simeq \frac{2\pi}{\lambda} \frac{\Delta x_\mathrm{p} X}{L} \tag{8}$$

and the interference figure is the well-known array of intense and sharp interference maxima at $X_\mathrm{n} = n(\lambda L)/(\Delta x_\mathrm{p})$, with $N-2$ smaller (by a factor of approximately N^2) peaks interposed (see Fig. 1 for reference). Expression (7) has to be multiplied by a Gaussian profile factor in order to take into account diffraction due to the finite dimensions of the sources in the real case. If d is the single-source width, then the width of the far-field interference pattern is of the order of $(\lambda L)/d$; accordingly, the number of main maxima in the interference pattern gives an indication of the ratio $(\Delta x_\mathrm{p})/d$ between the source spacing and the source width.

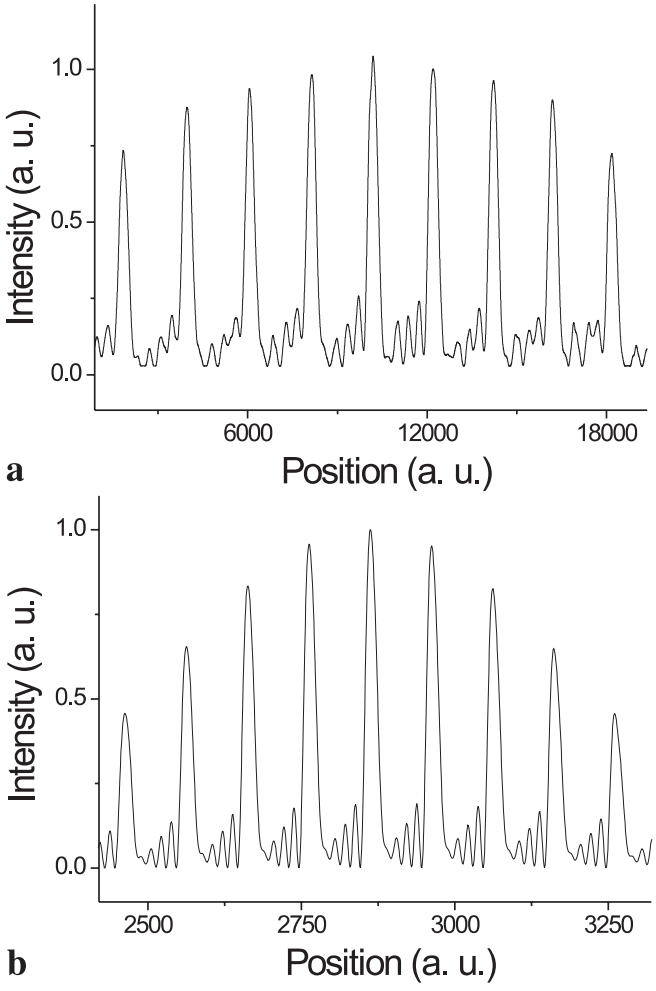

FIGURE 4 **a** Experimental profile of the multiple-supercontinuum-beam interference pattern as detected by scanning a photomultiplier in the far-field. Only the green part of the spectrum is selected by means of colored filters. **b** Calculation of the far-field interference pattern generated by an array of phase-locked supercontinuum sources under the same conditions of **a**. A relative phase, proportional to the laser intensity in the different filaments, is introduced in order to reproduce the experimental behavior of the secondary peaks

Figure 4a shows the experimental profile of the interference pattern produced by an array of white-light sources as seen by a scanning detector in the far field. The expected structure described by (7) is evident, with a clear array of strong interference maxima with smaller peaks interposed at regular distances. In this particular case, the laser pulse energy had been adjusted so that only 6 to 8 primary interference maxima reached the threshold intensity for supercontinuum generation. From the number of main maxima under the FWHM span of the interference profile, we estimate a ratio of about 10 between the source separations Δx_p and the source width d; accordingly, we can infer that the white-light sources are filaments with a diameter of the order of 10 μm or less.

Although the intensity distribution among the secondary maxima is not as regular as expected from the ideal case, it is nevertheless clear that only a smooth and slowly-varying phase must be present in the array of supercontinuum sources. In order to better reproduce the observed interference patterns, some phase distribution among the different supercon-

tinuum sources has to be introduced in the model. There are several possible justifications for the introduction of a relative phase among the sources, the main and simpler one being the fact that the different filaments come from laser interference maxima of different intensities. In the usual case of a positive nonlinear refraction index n_2, a laser intensity higher by ΔI provokes an increase of the effective optical path in the medium of thickness l, corresponding to a phase delay of

$$\Delta\varphi = \frac{2\pi}{\lambda} n_2 \Delta I l \tag{9}$$

Although we expect the intensity in the filaments to reach a common saturation value for the central peaks of the laser interference maxima, the supercontinuum sources placed at the wings of the distribution are generated by lower-intensity regions and thus suffer a smaller phase delay. It is reasonable to assume that the pump peak intensity distribution in the filaments is approximately given by (6), so that we can use this expression, together with (9), to estimate the phase distribution $\Delta\varphi(x)$ in the array.

If we consider a saturation intensity of about 10^{12}–10^{13} W/cm^2 in the central filaments, and a nonlinear refractive index n_2 for silica of the order of 3×10^{-16} cm^2/W, we find that a propagation distance of a few mm is sufficient to establish phase shifts of tens of radians between the central peaks and the outer ones. Moreover, small spatial asymmetries in the intensity distribution can easily account for the asymmetries observed in the far-field interference patterns. A simulated far-field pattern, obtained by fast fourier transformation of the source intensity-phase distributions given by (6) and (7), is shown in Fig. 4b for the situation corresponding to the experimental results of Fig. 4a. The qualitative agreement with the experimental data is evident.

When a higher laser pulse energy (of the order of 200 μJ per interfering pump pulse) is used, more pump interference maxima reach the threshold for white-light generation and more phase-locked sources are involved in the production of the far-field pattern. This situation is shown in the experimental interference pattern of Fig. 5, where about 15 supercontinua are active, corresponding to the source area image shown in Fig. 3. Interestingly, the distribution of intensity in the secondary maxima visible in Fig. 5 is much more irregular in this case, due to a more complicated phase distribution among the sources that probably arises from small inhomogeneities in the material or in the pump intensity profile.

Note, however, that also in this case the recorded profiles are extremely stable in time; exposure times of several seconds do not spoil the visibility of these multiple-beam interference patterns in a substantial way when a CCD camera is used to record the images. So, however complicated the phase distribution, it is essentially the same from shot to shot, with little perturbations due to laser intensity fluctuations.

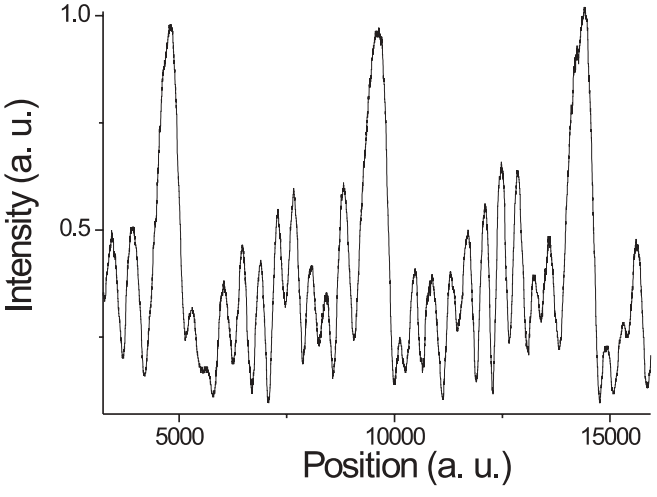

FIGURE 5 Same as Fig. 4 but with a higher pulse energy. More white-light sources (at least 15) are present with a more pronounced phase distribution which gives rise to distortions in the interference profile

4 Conclusions

We have generated a variable-spacing linear array of supercontinuum sources in bulk media and we have verified the preservation of their mutual phase coherence by studying far-field interference patterns. We have observed clear and stable interferences throughout all the visible spectrum, demonstrating the robustness of the white-light phase characteristics, which are preserved even in the presence of strong nonlinearities involved in the generation process. A simple model describing our experimental situation, involving the spatial interference pattern of two ultrashort laser pulses as a source for supercontinuum generation, was developed and its results compared to the observations. In particular, we found that both pump intensity clamping inside the filaments, and the inclusion of a pump-intensity-dependent relative phase among the different white-light sources were necessary in order to reproduce the finer details of the experimental multiple-source interference patterns. Although this phase distribution may assume complicated structures depending on the detailed dynamics of interaction between the laser pulses and the medium, the observation of stable interference patterns demonstrates that it is relatively constant in time and essentially immune to moderate intensity fluctuations of the laser pulse energy.

REFERENCES

1 R.R. Alfano, S.L. Shapiro: Phys. Rev. Lett. **24**, 584 (1970)
2 R.L. Fork, C.V. Shank, C. Hirlimann, R. Yen: Opt. Lett. **8**, 1 (1983)
3 P.B. Corkum, C. Rolland, T. Srinivasan-Rao: Phys. Rev. Lett. **57**, 2268 (1986)
4 F.A. Ilkov, L.S. Ilkova, S.L. Chin: Opt. Lett. **18**, 681 (1993)
5 R.R. Alfano: *The Supercontinuum Laser Source* (Springer-Verlag, New York 1989)
6 For a recent review see: *Special Issue on Supercontinuum*, Appl. Phys. B **77**, 2/3 (2003)
7 V.I. Klimov, D.W. McBranch: Opt. Lett. **23**, 277 (1998)
8 S.A. Kovalenko, A.L. Dobryakov, J. Ruthmann, N.P. Ernsting: Phys. Rev. A **59**, 2369 (1999)
9 R.L. Fork, C.H. Brito Cruz, P.C. Becker, C.V. Shank: Opt. Lett. **12**, 483 (1987)
10 E.T.J. Nibbering, O. Dühr, G. Korn: Opt. Lett. **22**, 1335 (1997)
11 V.V. Yakovlev, B. Kohler, K.R. Wilson: Opt. Lett. **19**, 2000 (1994)
12 M.K. Reed, M.K. Steiner-Shepard, D.K. Negus: Opt. Lett. **19**, 1885 (1994)
13 K.R. Wilson, V.V. Yakovlev: J. Opt. Soc. Am B **14**, 444 (1997)
14 G.Y. Yang, Y.R. Shen: Opt. Lett. **9**, 510 (1984)
15 W.L. Smith, P. Liu, N. Bloembergen: Phys. Rev. A **15**, 2396 (1977)

16 J. Ranka, R.W. Schirmer, A. Gaeta: Phys. Rev. Lett. **77**, 3783 (1996)
17 A. Brodeur, S.L. Chin: Phys. Rev. Lett. **80**, 4406 (1998)
18 A. Brodeur, S.L. Chin: J. Opt. Soc. Am. B **16**, 637 (1999)
19 A. Brodeur, F.A. Ilkov, S.L. Chin: Opt. Commun. **129**, 193 (1996)
20 W. Liu, S. Petit, A. Becker, N. Aközbek, C.M. Bowden, S.L. Chin: Opt. Commun. **202**, 189 (2002)
21 M. Bellini, T.W. Hänsch: Opt. Lett. **25**, 1049 (2000)
22 S.A. Diddams, D.J. Jones, J. Ye, S.T. Cundiff, J.L. Hall, J.K. Ranka, R.S. Windeler, R. Holzwarth, T. Udem, T.W. Hänsch: Phys. Rev. Lett. **84**, 5102 (2000)
23 J. Reichert, M. Niering, R. Holzwarth, M. Weitz, T. Udem, T.W. Hänsch: Phys. Rev. Lett. **84**, 3232 (2000)
24 M. Niering, R. Holzwarth, J. Reichert, P. Pokasov, T. Udem, M. Weitz, T.W. Hänsch, P. Lemonde, G. Santarelli, M. Abgrall, P. Laurent, C. Salomon, A. Clairon: Phys. Rev. Lett. **84**, 5496 (2000)
25 D.J. Jones, S.A. Diddams, J.K. Ranka, A. Stentz, R.S. Windeler, J.L. Hall, S.T. Cundiff: Sci. **288**, 635 (2000)
26 W. Watanabe, Y. Masuda, H. Arimoto, K. Itoh: Opt. Rev., **6**, 167 (1999)
27 W. Watanabe, K. Itoh: Jpn. J. Appl. Phys. **40**, 592 (2001)
28 C. Corsi, A. Tortora, M. Bellini: Appl. Phys. B **77**, 285 (2003)